



**HAL**  
open science

# Laboratory experiments of forced plumes in a density-stratified crossflow and implications for volcanic plumes

Guillaume Carazzo, Frédéric Girault, Thomas Aubry, H el ene Bouquerel,  
Edouard Kaminski

► **To cite this version:**

Guillaume Carazzo, Frédéric Girault, Thomas Aubry, H el ene Bouquerel, Edouard Kaminski. Laboratory experiments of forced plumes in a density-stratified crossflow and implications for volcanic plumes. *Geophysical Research Letters*, 2014, 41 (24), pp.8759-8766. 10.1002/2014GL061887 . insu-02920519

**HAL Id: insu-02920519**

**<https://insu.hal.science/insu-02920519>**

Submitted on 25 Aug 2020

**HAL** is a multi-disciplinary open access archive for the deposit and dissemination of scientific research documents, whether they are published or not. The documents may come from teaching and research institutions in France or abroad, or from public or private research centers.

L'archive ouverte pluridisciplinaire **HAL**, est destin ee au d ep ot et  a la diffusion de documents scientifiques de niveau recherche, publi es ou non,  emanant des  tablissements d'enseignement et de recherche fran ais ou  trangers, des laboratoires publics ou priv es.

## RESEARCH LETTER

10.1002/2014GL061887

## Key Points:

- Laboratory experiments simulate a volcanic plume rising in a windy atmosphere
- Increasing effect of wind leads to three dynamical regimes for the plume
- We present new relationships for estimating mass eruption rate from plume height

## Supporting Information:

- Readme
- Figures S1–S7 and Tables S1 and S2
- Movie S1
- Movie S2
- Movie S3

## Correspondence to:

G. Carazzo,  
carazzo@ipgp.fr

## Citation:

Carazzo, G., F. Girault, T. Aubry, H. Bouquereel, and E. Kaminski (2014), Laboratory experiments of forced plumes in a density-stratified crossflow and implications for volcanic plumes, *Geophys. Res. Lett.*, *41*, 8759–8766, doi:10.1002/2014GL061887.

Received 17 SEP 2014

Accepted 24 NOV 2014

Accepted article online 28 NOV 2014

Published online 16 DEC 2014

## Laboratory experiments of forced plumes in a density-stratified crossflow and implications for volcanic plumes

Guillaume Carazzo<sup>1</sup>, Frédéric Girault<sup>1,2</sup>, Thomas Aubry<sup>1,3,4</sup>,  
Hélène Bouquereel<sup>1</sup>, and Edouard Kaminski<sup>1</sup>

<sup>1</sup>Institut de Physique du Globe, Sorbonne Paris Cité, Université Paris Diderot, CNRS UMR 7154, Paris, France, <sup>2</sup>Now at Laboratoire de Géologie de l'ENS, PSL Research University-CNRS UMR 8538, Paris, France, <sup>3</sup>Département de Physique, École Normale Supérieure de Cachan, Cachan, France, <sup>4</sup>Now at Department of Earth, Ocean and Atmospheric Sciences, The University of British Columbia, Vancouver, British Columbia, Canada

**Abstract** The mass eruption rate feeding a volcanic plume is commonly estimated from its maximum height. Winds are known to affect the column dynamics causing bending and hence reducing the maximum plume height for a given mass eruption rate. However, the quantitative predictions including wind effects on mass eruption rate estimates are not well constrained. To fill this gap, we present a series of new laboratory experiments on forced plumes rising in a density-stratified crossflow. We identify three dynamical regimes corresponding to increasing effect of wind on the plume rise. The transition from one regime to another is governed by two dimensionless velocity scales defined as a function of source and environmental parameters. The results are found consistent with the conditions of historical eruptions and provide new empirical relationships to estimate mass eruption rate from plume height in windy conditions, leading to valuable tools for eruption risk assessment.

## 1. Introduction

Explosive volcanic eruptions produce dense mixtures of hot volcanic gas and pyroclasts at the vent that can rise up to several tens of kilometers in the atmosphere [Wilson, 1976]. During the ascent, the bulk density of the mixture is reduced as a result of turbulent entrainment and thermal expansion of cold atmospheric air [Woods, 1988]. Where the density of the mixture becomes lower than the density of the atmosphere, natural convection lifts the column until it reaches a level of neutral buoyancy (LNB) and spreads out laterally under the influence of high-altitude winds.

The maximum height reached by a volcanic column is a key parameter to assess in near real time the mass discharge rate feeding an eruption [e.g., Mastin *et al.*, 2009], which is used in turn to forecast the concentration of ash injected into the atmosphere [e.g., Kaminski *et al.*, 2011]. Low-altitude winds are known to affect the plume dynamics and reduce its maximum height for a given eruption flow rate by more vigorous entrainment [Bursik, 2001; Degruyter and Bonadonna, 2012; Woodhouse *et al.*, 2013; Suzuki and Koyaguchi, 2013; Mastin, 2014]. Understanding quantitatively the influence of atmospheric winds on a volcanic column is therefore crucial to improve the assessment of volcanic hazards related to explosive eruptions [Houghton *et al.*, 2014].

Theoretical and numerical studies show that for high eruption intensity and/or low wind velocity, the volcanic column forms a “strong” plume hardly affected by the wind field [Bonadonna and Phillips, 2003]. By contrast, for low eruption intensity and/or high wind velocity, the column bends over and forms a “weak” plume whose trajectory is strongly controlled by the wind strength and direction [Bursik, 2001]. Theoretical studies suggest that the strong/weak plume transition may be governed by the ratio of wind velocity to characteristic velocity scale of the plume [Devenish *et al.*, 2010; Degruyter and Bonadonna, 2012, 2013; Woodhouse *et al.*, 2013]. The two regimes have been observed during historical eruptions [Sparks *et al.*, 1997; Mastin, 2014], reproduced in laboratory experiments [Fan, 1967], and modeled theoretically [Bursik, 2001] and numerically [Suzuki and Koyaguchi, 2013]. Published laboratory experiments in relation with buoyant jets rising in a crossflow or in a calm environment are mostly dedicated to simulating either the strong plume regime of explosive volcanic columns [Carey *et al.*, 1988; Woods and Caulfield, 1992; Veitch and Woods, 2000; Kaminski *et al.*, 2005; Clarke *et al.*, 2009; Carazzo and Jellinek, 2012; Jessop and Jellinek, 2014] or the

weak plume regime of smokestack plumes in a uniform environment [Fan, 1967; Hewett et al., 1971; Hoult and Weil, 1972; Wright, 1977; Hwang and Chiang, 1986; Huq, 1997].

In this paper, we describe new laboratory experiments simulating turbulent forced plumes rising in a windy stratified environment. The experiments reproduce the strong and weak plume regimes, and exhibit a third behavior in which the jet is distorted by wind. We determine the source and environmental conditions that control regime transitions. We propose a single master curve that encompasses the three dynamical regimes to better determine the mass discharge rate feeding a volcanic plume from its observed maximum height. Our results are then tested against a data set of historical eruptions to discuss the consequences of this work for explosive volcanic plumes.

## 2. Methods

The experiments were conducted at ambient temperature in a 50 cm high, 100 cm long, and 40 cm large Plexiglas tank (Figure S1 in the supporting information). The tank was first filled with an aqueous NaCl solution with a linear density stratification. Linear density profiles were generated by filling the tank with 20 layers of salt solutions slowly introduced using a float made of eight tubes (1 mm in diameter) coated of foam paper and filled with sponge in order to minimize mixing across the density interfaces as the stratification develops [Carazzo and Jellinek, 2013]. Mean densities of the stratified water were obtained by optical refractometer measurements of selective fluid samples collected with hypodermic tubing of 0.1 cm internal diameter. Density profiles were linear in each experiment except near the top and the bottom of the tank (Figure S2 in the supporting information). Prior to an experiment, a constant head tank located 3 m above the floor was filled with salt water using a pump connected to a larger reservoir (Figure S1 in the supporting information). The density of the injected mixture, measured with the same technique as the water in the tank, was systematically intermediate between those of the salt water at the bottom and at the top of the tank.

At the start of an experiment, we towed the jet source at a constant speed ( $3 \times 10^{-3}$  to  $6 \times 10^{-2}$  m s<sup>-1</sup>) through the stationary fluid, and we opened the valve allowing the jet fluid to be released downward from the water surface. The jet exit was a straight pipe with a 5.5 mm inner radius located 2 cm below the top water level of 42 cm, hence allowing the turbulent jet to reach a maximum height of 40 cm. The volumetric flow rate of the salt water, measured using an electromagnetic flowmeter, was maintained constant during an entire given experiment, but varied between  $1.4 \times 10^{-5}$  and  $10^{-4}$  m<sup>3</sup> s<sup>-1</sup> from one experiment to another. An injection lasted between 10 and 60 s and was recorded using a video camera (25 frames per second).

The density of the jet at the source, its volumetric flow rate, the strength of the density stratification, and the lateral speed of the injector (i.e., the speed of the crossflow) were varied from one experiment to another in order to cover the full range of conditions appropriate for a consistent scaling of natural volcanic plumes. Run conditions of the 32 experiments are compiled in Table S1 in the supporting information. To ensure experimental jets adequately scale to volcanic plumes and to compare our results with previous studies, we calculated a number of dimensionless parameters controlling the jet dynamics and compared the experimental values to those of natural volcanic plumes.

The Reynolds number ( $Re_0$ ) characterizes the ratio between inertial to viscous forces,

$$Re_0 = \frac{U_0 R_0}{\nu}, \quad (1)$$

where  $U_0$  and  $R_0$  are the jet velocity and radius at the source, respectively, and  $\nu$  is the kinematic viscosity of the fluid. In explosive eruptions,  $10^7 \leq Re_0 \leq 10^9$ , which is unattainable under laboratory conditions. We note, however, that our flows are at high  $Re$  (Table S1 in the supporting information), fully turbulent, and conducted under  $Re$  conditions comparable to many published studies [Burgisser et al., 2005; Carazzo and Jellinek, 2012].

The Richardson number at the source ( $Ri_0$ ) characterizes the balance between the buoyancy and inertial forces in the jet and can be written as

$$Ri_0 = \frac{g'_0 R_0}{U_0^2}, \quad (2)$$

where  $g'_0 = g(\rho_a - \rho_0)/\rho_a$  is the jet reduced gravity at the source, with  $g$  the acceleration of gravity, and  $\rho_0$  and  $\rho_a$  the densities of the jet and ambient fluid at the source, respectively. The source Richardson number is related to the source parameter ( $\Gamma$ ) introduced by Morton [1959] as  $Ri_0 = 4\alpha_p\Gamma/5$ , where  $\alpha_p = 0.125$  is the “top-hat” entrainment coefficient for a self-similar pure plume [Wang and Law, 2002; Carazzo et al., 2006]. The Richardson number (or the source parameter) fully characterizes the behavior of a pure plume in a uniform environment. In a stratified environment and in a crossflow, two additional dimensionless numbers are introduced.

For the purpose of comparing the source velocity imposed in our experiments ( $U_0$ ) with the characteristic velocity of a pure plume ( $NH_0$ ), we first introduce the plume velocity ratio,

$$U^* = \frac{NH_0}{U_0}, \quad (3)$$

where  $H_0 = \alpha_p^{-1/2} F_0^{1/4} N^{-3/4}$  is the natural length scale for a pure plume rising in a calm stratified environment [Morton et al., 1956], with  $F_0$  the source buoyancy flux, and  $N$  the Brunt-Väisälä frequency defined as

$$N^2 = -\frac{g}{\rho_r} \frac{d\rho}{dz}, \quad (4)$$

where  $\rho_r$  is a reference density, and  $z$  is the vertical distance from the bottom of the tank.

The plume velocity ratio ( $U^*$ ) is found to vary between 0.05 and 1 in natural volcanic plumes [Carazzo and Jellinek, 2012], as in our laboratory jet experiments (Table S1 in the supporting information), whereas  $U^* = 0$  in all previous laboratory studies performed in a uniform environment [Fan, 1967; Hewett et al., 1971; Hoult and Weil, 1972; Wright, 1977; Hwang and Chiang, 1986; Huq, 1997; Yang and Hwang, 2001]. Hence, our experiments are better analog for volcanic plumes, which do rise in a stratified atmosphere.

The presence of a crossflow introduces an additional velocity scale ( $W$ ), which defines the wind velocity ratio [Hewett et al., 1971; Yang and Hwang, 2001],

$$W^* = \frac{W}{U_0}, \quad (5)$$

where  $W$  is the velocity of the crossflow. Combining equations (3) and (5), and replacing  $H_0$  by its definition, gives an alternative choice for the third dimensionless velocity  $\alpha_p^{1/2} W / (F_0 N)^{1/4}$  that is commonly proposed to characterize the influence of wind on the plume dynamics [Devenish et al., 2010; Degruyter and Bonadonna, 2012; Woodhouse et al., 2013; Mastin, 2014].

Figure 1 shows that our experimental range of wind velocity ratio ( $W^*$ ) is consistent with values calculated for volcanic plumes [Carazzo and Jellinek, 2012]. The Richardson number at the base of volcanic jets is negative because the eruptive mixture is denser than the atmosphere at the vent, but its value increases rapidly and becomes positive due to entrainment and mixing of cold atmospheric air (Figure S3 in the supporting information). Although our laboratory experiments do not strictly reproduce the region of buoyancy inversion, our experimental range of  $Ri_0$  is consistent with values calculated for the buoyant region of volcanic plumes (Figure 1). The strength of the crossflow and the balance between the buoyancy and inertial forces acting on volcanic plumes are thus well reproduced at the laboratory scale. Whereas experimental work published in relation with buoyant jets in a uniform crossflow focus either on high- $Ri_0$  plumes in a strong (high- $W^*$ ) crossflow [Hewett et al., 1971; Hoult and Weil, 1972], or on low- $Ri_0$  plumes in a weak (low- $W^*$ ) crossflow [Fan, 1967; Huq, 1997; Yang and Hwang, 2001], our laboratory conditions cover relatively large ranges of  $Ri_0$  and  $W^*$  values (Figure 1).

### 3. Results

Our experiments investigate the behavior of the turbulent jet as we vary the source volumetric flow rate, the jet density at the source, the strength of the stratification in the tank, and the wind velocity. Thereafter, we describe the jet development as if the jet is rising, not falling. For low wind velocities and relatively high flow rates, the jet mixes with the ambient salt water (Movie S3 in the supporting information) and its density decreases as a result of turbulent entrainment and dilution to values lower than the ambient density. Resultant negative buoyancy forces reduce the momentum imparted at the source, and the force balance

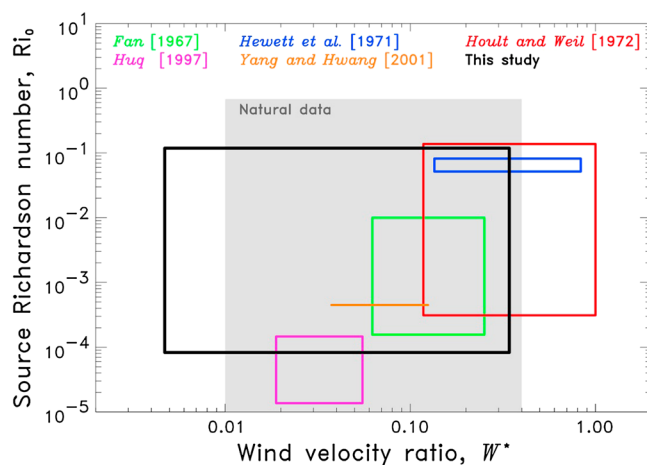


**Figure 1.** Review of source Richardson number ( $Ri_0$ ) and wind velocity ratio ( $W^*$ ) for natural volcanic plumes and experimental works published in relation with buoyant jets in a crossflow. The values of  $Ri_0$  for natural data correspond to those of the buoyant region of volcanic plumes.

drives the plume to a level of neutral buoyancy (LNB), which it overshoots to a maximum height. The jet then collapses back to the LNB as a fountain and spreads out laterally under the influence of the crossflow to form an umbrella cloud. The spreading umbrella reaches a stagnation point upwind where the radial expansion velocity is equal to the wind speed. This behavior is shown in Figure 2a (experiment 25) and is a laboratory analog of a strong Plinian plume [Bonadonna and Phillips, 2003].

For high wind velocities and relatively low flow rates, the jet mixes more efficiently than in the strong plume case by ingesting significant quantities of ambient salt water through the action of wind (Movie S1 in the supporting information). The centerline of the jet bends over in the wind field, and the jet starts spreading subhorizontally around the LNB. This behavior is shown in Figure 2c (experiment 24) and is a laboratory analog of a weak plume [Bursik, 2001].

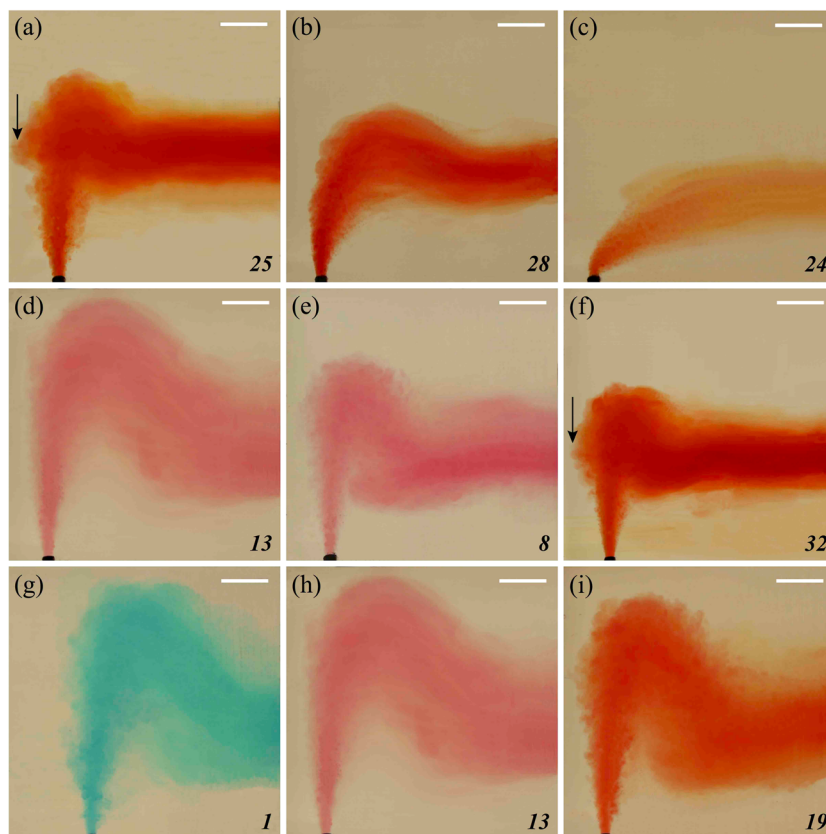


**Figure 2.** Photographs of the experiments illustrating the effects on the plume rise of increasing the wind velocity ratio: (a)  $W^* = 0.076$ ; (b)  $W^* = 0.171$ ; (c)  $W^* = 0.402$ ; increasing the source Richardson number: (d)  $Ri_0 = 8.4 \times 10^{-4}$ ; (e)  $Ri_0 = 3.5 \times 10^{-3}$ ; (f)  $Ri_0 = 2.9 \times 10^{-2}$ ; and increasing the strength of the stratification: (g)  $N = 0.3 \text{ s}^{-1}$ ; (h)  $N = 0.5 \text{ s}^{-1}$ ; (i)  $N = 0.7 \text{ s}^{-1}$ . All the scale bars are 5 cm long. Numbers correspond to the experiment numbers reported in Table S1 in the supporting information. Arrows indicate the stagnation point reached by strong plumes.

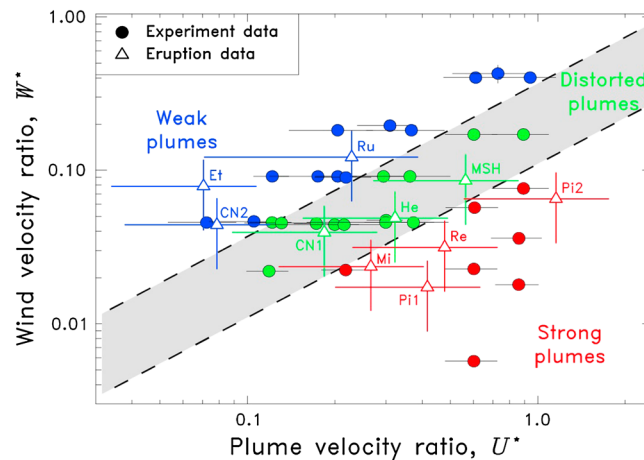


**Figure 3.** Regime diagram of the wind velocity ratio ( $W^*$ ) as a function of the plume velocity ratio ( $U^*$ ) for all the experiments. Red, green, and blue symbols correspond to plumes in the strong, distorted, and weak regime, respectively ( $1\sigma$  error bar). Dashed lines give experimental transitions between the regimes. Open triangles correspond to natural eruptions: CN1 = Cerro Negro, 9–12 April 1992; CN2 = Cerro Negro, November–December 1995; Et = Etna, 19–24 July 2001; He = Hekla, 17 August 1980; Mi = Miyakejima, 18 August 2000; MSH = Mount St. Helens, 18 May 1980; Pi1 = Pinatubo, 12 June 1991; Pi2 = Pinatubo, 15 June 1991; Re = Reventador, 3 November 2002; Ru = Ruapehu, 17 June 1996 (see Table S2 in the supporting information).

For intermediate wind velocities and moderate flow rates, there is less entrainment and mixing of the ambient fluid due to wind than in the weak plume case, but the centerline of the jet is still distorted (Movie S2 in the supporting information). As in the strong plume regime, the jet reaches a maximum height before it collapses to a LNB. However, by contrast with strong plumes which exhibit a stagnation point upwind and with weak plumes that may slightly oscillate around their LNB with downwind distance from the source, here, the umbrella cloud is carried off by the wind field and no stagnation point develops, and the plume collapses to the LNB within a downwind distance of one plume height. This behavior is shown in Figure 2d (experiment 13) and has not been recognized in previous laboratory studies. We refer thereafter to this behavior as the “distorted” plume regime.

Figure 2 illustrates the influence of the main source and environmental parameters on the behavior of the buoyant jet. Increasing the wind velocity ratio  $W^*$ , either by increasing the lateral speed of the injector or decreasing the source plume velocity, strongly affects the trajectory of the jet, which may pass from one dynamical regime to another, and reduces the maximum height by up to a factor of 2 (Figures 2a–2c). The source Richardson number (Figures 2d–2f) and the strength of the stratification (Figures 2g–2i) have both less influence on the behavior of the jet and cannot be used to discriminate the conditions favorable for the formation of a strong, distorted, or weak plume.

The evolution of the buoyant jet strongly depends on the evolution of its density relative to the environment, which is governed by turbulent entrainment. The rate of entrainment of ambient fluid in the jet is controlled by the vertical plume velocity [Morton *et al.*, 1956] and the horizontal wind velocity [Hewett *et al.*, 1971], suggesting that the plume velocity ratio ( $U^*$ ) and the wind velocity ratio ( $W^*$ ) are key parameters to characterize the behavior of the jet. Figure 3 shows that the threshold conditions separating the strong and distorted regimes, and the distorted and weak plume regimes, are actually straight lines with a slope of  $0.11 \pm 0.01$  and  $0.37 \pm 0.03$ , respectively. In cases where  $W^*/U^* < 0.11$  the turbulent jet forms a strong plume, whereas for  $W^*/U^* > 0.37$  a weak plume develops. Distorted plumes form for intermediate conditions given by  $0.11 \leq W^*/U^* \leq 0.37$ . These results show that the ratio  $W^*/U^* = \alpha_p^{1/2} W / (F_0 N)^{1/4}$  can fully describe the transition from one regime to another, consistent with previous theoretical works on the weak/strong plume transition [Devenish *et al.*, 2010; Degruyter and Bonadonna, 2012; Woodhouse *et al.*, 2013; Mastin, 2014].

The maximum height reached by the buoyant jet varies a lot from one dynamical regime to another. To quantitatively characterize the impact of wind on this height, we calculated the ratio of the imposed volumetric flow rate in our experiments ( $Q$ ) to the volumetric flow rate required to reach the same maximum height under no wind conditions ( $Q_0$ ). The latter parameter is calculated using a 1-D model of turbulent jet [Morton *et al.*, 1956] with variable entrainment [Kaminski *et al.*, 2005]. The dimensionless volumetric flow rate  $Q/Q_0$  is found to be close to 1 in strong plumes, and close to 10 in weak plumes. Comparing  $Q/Q_0$  with the dimensionless number  $W^*/U^*$  shows that the latter parameter cannot be used to quantify the impact of wind on plume height (Figure S4 in the supporting information). To make a link between  $Q/Q_0$  and the previously described regimes, we assume that the  $Q/Q_0$  ratio is controlled by the plume distortion during its rise. To characterize this distortion, we follow a simple kinetic approach and introduce the ratio between the

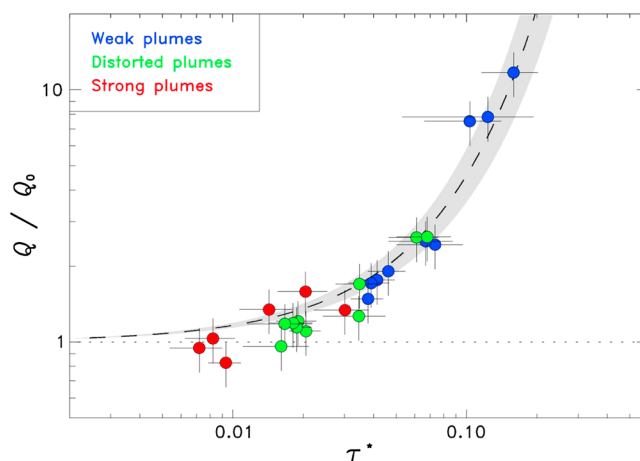


**Figure 4.** Dimensionless volumetric flow rate  $Q/Q_0$  as a function of the dimensionless time scale  $\tau^*$  (see text) in our experiments. Dashed line corresponds to the best fit exponential curve given by  $\ln(Q/Q_0) = a\tau^*$ , with  $a = 15.2 \pm 2.5$  (uncertainty as grey envelope). The coefficient of determination is  $R^2 = 0.93 \pm 0.06$ .

time scale of horizontal motions is much larger than the one of vertical motions, wind effects are expected to be negligible and the plume not to be distorted (i.e.,  $Q/Q_0$  tends to unity). Figure 4 confirms these expectations and shows that all data collapse onto a single master curve given by  $\ln(Q/Q_0) = a\tau^*$ , with  $a = 15.2 \pm 2.5$ .

#### 4. Implications for Volcanic Plumes

We have shown that buoyant jets rising in a crossflow may form either strong, distorted, or weak plumes depending on the source and environmental conditions characterized by the wind velocity ratio  $W^*$  and the plume velocity ratio  $U^*$ . Despite this variety of regimes, the maximum height reached by the jet can be predicted by using a single master curve. We now test these results against natural data of explosive volcanic eruptions.

To quantify the impact of wind on a volcanic plume, we estimated the wind and plume velocity ratios of well-documented eruptions. For this, we used information about the mass discharge rate (MDR), the average wind velocity, and average stratification frequency that can be found in the literature. Mass discharge rates were determined independently (i.e., not from the column height) using information on the total eruption volume and duration [Mastin *et al.*, 2009; Girault *et al.*, 2014]. Wind velocities and stratification frequencies correspond to average values given by Mastin [2014] (see Table S2 in the supporting information). We assume that the gas and particles are strongly coupled in the plume, there is no humidity in the atmosphere, and there is no strong overpressure at the base of the column. These assumptions are valid for most Plinian eruptions (see Girault *et al.* [2014] for a detailed discussion), although the influence of overpressure can be important in some cases [Ogden, 2011; Saffaraval *et al.*, 2012]. Figure 3 compares the predictions of the experimentally determined transitions with our estimated values for  $W^*$  and  $U^*$  from natural data. The consistency between the predictions and the data demonstrates that the threshold conditions separating the different regimes in our experiments capture the behavior of volcanic plumes. These predictions may therefore be used as a simple tool to predict at first order the evolution of a volcanic plume rising in a wind field.

The results presented in Figure 4 suggest that where winds are negligible ( $\tau^* \rightarrow 0$ ), the mass discharge rate feeding a volcanic plume can be inferred from its maximum height by using the classical scaling relationship valid for no wind conditions (i.e.,  $MDR = MDR_0$ ). In the limit of extreme wind conditions ( $\tau^* \geq 0.1$ ), the calculated mass discharge rate can be significantly lower and may be as low as one tenth of its actual value (Figure 4). Comparing our experimental results with the predictions made by 1-D models of a volcanic plume in a crossflow suggests that the new scaling relationship drawn in Figure 4 captures the physics of the phenomenon (Figure S5 in the supporting information). Combining this relationship with the results of Carazzo *et al.* [2008] on volcanic plumes rising in a calm environment, we propose the following

two time scales for the key dynamics at work

$$\tau^* = \frac{\tau_v}{\tau_h}, \quad (6)$$

where  $\tau_v = H_0/U_0$  is the time scale of vertical motions of a parcel of fluid in the plume and  $\tau_h = H_1/W$  is the time scale of horizontal motions of the parcel of fluid in the plume induced by the wind. Here the length scale  $H_1$  is the reference depth (or altitude) over which the wind acts (e.g., the tank depth in our experiments or the tropopause height in the atmosphere). For  $\tau^* \gg 1$ , the time scale of horizontal motions is small, wind effects are expected to be dominant and the plume to be strongly distorted (i.e.,  $Q/Q_0$  is large). For  $\tau^* \ll 1$ , the

extended relationships to estimate the mass discharge rate MDR (in  $\text{kg s}^{-1}$ ) from the observed maximum column height  $H_{\text{obs}}$  (in km):

$$\ln(\text{MDR}) = \ln(b_1 H_{\text{obs}}^{n_1}) + (cWH_{\text{obs}}) \quad \text{for } H_{\text{obs}} \leq H_1 \quad (7)$$

$$\ln(\text{MDR}) = \ln(b_2 H_{\text{obs}}^{n_2}) + (cWH_{\text{obs}}) \quad \text{for } H_1 < H_{\text{obs}} \leq H_2 \quad (8)$$

$$\ln(\text{MDR}) = \ln(b_3 H_{\text{obs}}^{n_3}) + (cWH_{\text{obs}}) \quad \text{for } H_2 < H_{\text{obs}} \leq H_3 \quad (9)$$

$$\ln(\text{MDR}) = \ln(b_4 H_{\text{obs}}^{n_4}) + (cWH_{\text{obs}}) \quad \text{for } H_{\text{obs}} > H_3 \quad (10)$$

where  $W$  is the wind velocity (in  $\text{m s}^{-1}$ ) at the tropopause height [Woodhouse *et al.*, 2013],  $b_1 = 142.14$ ,  $b_2 = 2.21$ ,  $b_3 = 46.73$ ,  $b_4 = 1928.8$ ,  $n_1 = 4.04$ ,  $n_2 = 5.86$ ,  $n_3 = 4.72$ ,  $n_4 = 3.47$ ,  $c = 0.0031$ ,  $H_1 = 10$  km,  $H_2 = 14$  km,  $H_3 = 20$  km for polar atmospheric conditions,  $b_1 = 59.61$ ,  $b_2 = 0.0014$ ,  $b_3 = 0.198$ ,  $b_4 = 429.2$ ,  $n_1 = 4.05$ ,  $n_2 = 7.78$ ,  $n_3 = 6.18$ ,  $n_4 = 3.84$ ,  $c = 0.0016$ ,  $H_1 = 17$  km,  $H_2 = 21$  km,  $H_3 = 26$  km for tropical atmospheric conditions, and  $b_1 = 63.22$ ,  $b_2 = 0.061$ ,  $b_3 = 4.41$ ,  $b_4 = 653.81$ ,  $n_1 = 4.06$ ,  $n_2 = 6.89$ ,  $n_3 = 5.38$ ,  $n_4 = 3.75$ ,  $c = 0.0025$ ,  $H_1 = 11.5$  km,  $H_2 = 17$  km,  $H_3 = 21$  km for midlatitude atmospheric conditions. The calculations reported in Carazzo *et al.* [2008] were made for a magma temperature of 1200 K, a specific heat of the volcanic gas and solid particles of  $2000 \text{ J K}^{-1} \text{ kg}^{-1}$  and  $1617 \text{ J K}^{-1} \text{ kg}^{-1}$ , respectively, and for three different atmospheric profiles. Testing these relationships with data on natural plumes (Table S2 in the supporting information) reveals a good agreement between the predicted and measured mass discharge rates (Figure S6 in the supporting information). A comparison of these relationships with previous scaling laws [Degruyter and Bonadonna, 2012; Woodhouse *et al.*, 2013] shows that all the models converge in the absence of wind but do not agree in windy conditions (Figure S7 in the supporting information), most likely because the intensity of turbulent entrainment due to wind is poorly constrained and varies from one study to another. Thus, our experimental results open new perspectives to quantitatively determine how the presence of wind affects turbulent entrainment in the plume.

## 5. Conclusion

We have presented a series of laboratory experiments simulating a buoyant jet rising in a stratified environment under a uniform crossflow. We show that depending on the environmental and source conditions, the buoyant jet follows three distinct dynamical regimes: strong, distorted, and weak plume. The transition from one dynamical regime to another depends on the ratios of the three different velocity scales of the problem: the source velocity, a pure plume velocity scale depending on the strength of the stratification, and the wind velocity. The transitions between the three regimes found in the experiments are consistent with the conditions of historical eruptions. The experiments illustrate how the mass discharge rate inferred from the maximum height of a volcanic plume can be reduced under strong wind conditions by up to an order of magnitude compared to its actual value. The new formulae presented in this study to link the mass discharge rate to the maximum column height can be used to efficiently assess volcanic hazards, especially during the management of eruptive crises that require simple, robust, and fast predictions.

### Acknowledgments

The paper benefited from thorough comments by Larry Mastin, an anonymous reviewer, and the Associate Editor. Support was provided by the Institut National des Sciences de l'Univers (INSU-CNRS). Data supporting Figure 3 are available as Tables S1 and S2 in the supporting information. Data supporting this article are available as Figures S1–S7 and Movies S1–S3 in the supporting information.

The Editor thanks Larry Mastin and an anonymous reviewer for their assistance in evaluating this paper.

### References

- Bonadonna, C., and J. C. Phillips (2003), Sedimentation from strong volcanic plumes, *J. Geophys. Res.*, *108*(B7), 2340, doi:10.1029/2002JB002034.
- Burgisser, A., G. W. Bergantz, and R. E. Breidenthal (2005), Addressing complexity in laboratory experiments: The scaling of dilute multiphase flows in magmatic systems, *J. Volcanol. Geotherm. Res.*, *141*, 245–265.
- Bursik, M. (2001), Effect of wind on the rise height of volcanic plumes, *Geophys. Res. Lett.*, *28*, 3621–3624, doi:10.1029/2001GL013393.
- Carazzo, G., and A. M. Jellinek (2012), A new view of the dynamics, stability and longevity of volcanic clouds, *Earth Planet. Sci. Lett.*, *325–326*, 39–51.
- Carazzo, G., and A. M. Jellinek (2013), Particle sedimentation and diffusive convection in volcanic ash-clouds, *J. Geophys. Res. Solid Earth*, *118*, 1420–1437, doi:10.1002/jgrb.50155.
- Carazzo, G., E. Kaminski, and S. Tait (2006), The route to self-similarity in turbulent jets and plumes, *J. Fluid Mech.*, *547*, 137–148.
- Carazzo, G., E. Kaminski, and S. Tait (2008), On the rise of turbulent plumes: Quantitative effects of variable entrainment for submarine hydrothermal vents, terrestrial and extra terrestrial explosive volcanism, *J. Geophys. Res.*, *113*, B09201, doi:10.1029/2007JB005458.
- Carey, S., H. Sigurdsson, and R. S. J. Sparks (1988), Experimental studies of particle-laden plumes, *J. Geophys. Res.*, *93*, 15,314–15,328, doi:10.1029/JB093iB12p15314.
- Clarke, A. B., J. C. Phillips, and K. N. Chojnicki (2009), An investigation of Vulcanian eruption dynamics using laboratory analogue experiments and scaling analysis, in *Studies in Volcanology: The Legacy of George Walker. Spec. Publ. of IAVCEI*, vol. 2, edited by T. Thordarson *et al.*, pp. 155–166, Geol. Soc. London, London, U. K.

- Degruyter, W., and C. Bonadonna (2012), Improving on mass flow rate estimates of volcanic eruptions, *Geophys. Res. Lett.*, *39*, L16308, doi:10.1029/2012GL052566.
- Degruyter, W., and C. Bonadonna (2013), Impact of wind on the condition for column collapse of volcanic plumes, *Earth Planet. Sci. Lett.*, *377–378*, 218–226.
- Devenish, B. J., G. G. Rooney, H. N. Webster, and D. J. Thomson (2010), The entrainment rate for buoyant plumes in a crossflow, *Boundary Layer Meteorol.*, *134*, 411–439.
- Fan, L.-N. (1967), Turbulent buoyant jets into stratified or flowing ambient fluids, *Tech. Rep. KH-R-15*, W. M. Keck Laboratory of Hydrology and Water Resources, California Institute of Technology, Pasadena, Calif.
- Girault, F., G. Carazzo, S. Tait, F. Ferrucci, and E. Kaminski (2014), The effect of total grain-size distribution on the dynamics of turbulent volcanic plumes, *Earth Planet. Sci. Lett.*, *394*, 124–134.
- Hewett, T. A., J. A. Fay, and D. P. Hoult (1971), Laboratory experiments of smokestack plumes in a stable atmosphere, *Atmos. Environ.*, *5*, 767–789.
- Houghton, B. F., R. J. Carey, and M. D. Rosenberg (2014), The 1800a Taupo eruption: “Ill wind” blows the ultraplinian type event down to Plinian, *Geology*, *42*, 459–461.
- Hoult, D. P., and J. C. Weil (1972), Turbulent plume in a laminar cross flow, *Atmos. Environ.*, *6*, 513–531.
- Huq, P. (1997), Observations of jets in density stratified crossflows, *Atmos. Environ.*, *31*, 2011–2022.
- Hwang, R. R., and T. P. Chiang (1986), Buoyant jets in a crossflow of stably stratified fluid, *Atmos. Environ.*, *20*, 1887–1890.
- Jessop, D. E., and A. M. Jellinek (2014), Effects of particle mixtures and nozzle geometry on entrainment into volcanic jets, *Geophys. Res. Lett.*, *41*, 3858–3863, doi:10.1002/2014GL060059.
- Kaminski, E., S. Tait, and G. Carazzo (2005), Turbulent entrainment in jets with arbitrary buoyancy, *J. Fluid Mech.*, *526*, 361–376.
- Kaminski, E., S. Tait, F. Ferrucci, M. Martet, B. Hirn, and P. Husson (2011), Estimation of ash injection in the atmosphere by basaltic volcanic plumes: The case of the Eyjafjallajökull 2010 eruption, *J. Geophys. Res.*, *116*, B00C02, doi:10.1029/2011JB008297.
- Mastin, L. G. (2014), Testing the accuracy of a 1-D volcanic plume model in estimating mass eruption rate, *J. Geophys. Res. Atmos.*, *119*, 2474–2495, doi:10.1002/2013JD020604.
- Mastin, L. G., et al. (2009), A multidisciplinary effort to assign realistic source parameters to models of volcanic ash-cloud transport and dispersion during eruptions, *J. Volcanol. Geotherm. Res.*, *186*, 10–21.
- Morton, B. R. (1959), Forced plumes, *J. Fluid Mech.*, *5*, 151–163.
- Morton, B. R., G. I. Taylor, and J. S. Turner (1956), Turbulent gravitational convection from maintained and instantaneous source, *Philos. Trans. R. Soc. A*, *234*, 1–23.
- Ogden, D. (2011), Fluid dynamics in explosive volcanic vents and craters, *Earth Planet. Sci. Lett.*, *312*, 401–410.
- Saffaraval, F., S. A. Solovitz, D. E. Ogden, and L. G. Mastin (2012), Impact of reduced near-field entrainment of overpressured volcanic jets on plume development, *J. Geophys. Res. Solid Earth*, *117*, B05209, doi:10.1029/2011JB008862.
- Sparks, R. S. J., M. Bursik, S. Carey, J. S. Gilbert, L. S. Glaze, H. Sigurdsson, and A. W. Woods (Eds.) (1997), *Volcanic Plumes*, John Wiley, New York.
- Suzuki, Y. J., and T. Koyaguchi (2013), 3D numerical simulation of volcanic eruption clouds during the 2011 Shinmoe-dake eruptions, *Earth Planets Space*, *65*, 581–589.
- Veitch, G., and A. W. Woods (2000), Particle recycling and oscillations of volcanic eruption columns, *J. Geophys. Res.*, *105*, 2829–2842, doi:10.1029/1999JB900343.
- Wang, H., and A. W.-K. Law (2002), Second-order integral model for a round turbulent buoyant jet, *J. Fluid Mech.*, *459*, 397–428.
- Wilson, L. (1976), Explosive volcanic eruptions—III. Plinian eruption columns, *Geophys. J. R. Astron. Soc.*, *45*, 543–556.
- Woodhouse, M. J., A. J. Hogg, J. C. Phillips, and R. S. J. Sparks (2013), Interaction between volcanic plumes and wind during the 2010 Eyjafjallajökull eruption, Iceland, *J. Geophys. Res. Solid Earth*, *118*, 92–109, doi:10.1029/2012JB009592.
- Woods, A. W. (1988), The fluid dynamics and thermodynamics of eruption columns, *Bull. Volcanol.*, *50*, 169–193.
- Woods, A. W., and C. P. Caulfield (1992), A laboratory study of explosive volcanic eruptions, *J. Geophys. Res.*, *97*, 6699–6712, doi:10.1029/92JB00176.
- Wright, S. J. (1977), Mean behavior of buoyant jets in a crossflow, *J. Hydraul. Div.*, *103*(5), 499–513.
- Yang, W.-C., and R. R. Hwang (2001), Vertical buoyant jets in a linearly stratified ambient cross-stream, *Environ. Fluid Mech.*, *1*, 235–256.